ACTA ASTRONOMICA
Vol. **66** (2016) pp. 357–379

CCD Photometry, Roche Modeling and Evolutionary History of the W UMa-type Eclipsing Binary TYC 01664-0110-1

K. B. Alton[1] and K. Stępień[2]

[1] UnderOak Observatory, Cedar Knolls, NJ 07927, USA
e-mail: mail@underoakobservatory.com
[2] Warsaw University Observatory, Al. Ujazdowskie 4, 00-478 Warszawa, Poland
e-mail: kst@astrouw.edu.pl

Received August 17, 2016

ABSTRACT

TYC 01664-0110-1 (ASAS J212915+1604.9), a W UMa-type variable system ($P = 0.282962$ d), was first detected over 17 years ago by the ROTSE-I telescope. Photometric data (*B, V* and I_c) collected at UnderOak Observatory (UO) resulted in five new times-of-minima for this variable star which were used to establish a revised linear ephemeris. No published radial velocity (*RV*) data are available for this system. However, since this W UMa binary undergoes a total eclipse, Roche modeling based on the Wilson-Devinney (W-D) code yielded a well-constrained photometric value for M_2/M_1 ($q = 0.356 \pm 0.001$). There is a suggestion from ROTSE-I (1999) and ASAS survey data (2003, 2005, and 2008) that the secondary maximum is more variable than the primary one probably due to the so-called O'Connell effect. However, peak asymmetry in light curves (LC) from 2015 was barely evident during quadrature. Therefore, W-D model fits of these most recent data did not yield any substantive improvement with the addition of spot(s).

Using the evolutionary model of cool close binaries we searched for a possible progenitor of TYC 01664-0110-1. The best fit is obtained if the initial binary has an orbital period between 3.3–3.8 d and component masses between 1.0–1.1 $M_\odot$ and 0.30–0.35 $M_\odot$. The model progenitor needs about 10 Gyr to attain the presently observed parameters of the variable. Its period slowly increases and the mass ratio decreases. According to the model predictions TYC 01664-0110-1 will go through the common envelope (CE) phase in the future, followed by merging of both components or formation of a double degenerate.

Due to its apparent brightness ($m_{V,\max} \approx 10.9$ mag) and unique properties, the star is an excellent target for spectroscopic investigation of any possible deviations from a simple static model of a contact binary.

Key words: *binaries: eclipsing – starspots – Stars: evolution*

1. Introduction

Low mass contact binaries (LMCB) represent a subset of W UMa-type variables which have orbital periods shorter than 0.3 d and a total mass under 1.4 $M_\odot$. In general the more massive star in an LMCB is cooler than its binary cohort and is classified as a W-type variable according to Binnendijk (1970). Models suggest that cool contact binaries start as detached binaries with orbital periods of a

few days and evolve inward by the angular momentum loss (AML) associated with magnetized winds (Stępień 2006, 2011a). In this evolutionary scenario, changes in orbital period are attributed to a balance between mass transfer from the less massive star to its companion which expands the orbital distance and AML loss from the wind which tightens the orbital radius. The variable behavior of TYC 01664-0110-1 was first observed in 1999 during the ROTSE-I CCD survey (Woźniak *et al.* 2004, Gettel *et al.* 2006) and the system later classified by Hoffman *et al.* (2009). Photometric data (*V*-mag) for TYC 01664-0110-1 were also captured by the All Sky Automated Survey (ASAS, Pojmański *et al.* 2005). Pilecki and Stępień (2012) further studied this system with a subset of other LMCBs which were modeled using Monte Carlo simulation and the W-D code. This variable star was also included in a BVR_cI_c survey (Terrell *et al.* 2012) designed to provide accurate colors for a large population of W UMa eclipsing binaries brighter than 14 mag. During an investigation of the superWASP survey of stars, Lohr *et al.* (2015) uncovered period variations which suggested a positive linear change (0.059 s/yr) in orbital period.

Here we analyze new photometric data obtained by one of us (KBA). The revised set of binary parameters is obtained from the LC solution and the absolute values for component masses and radii derived. Based on these values, the progenitor model of TYC 01664-0110-1 was found and its evolution traced from zero age main sequence (ZAMS) till the present state. The future fate is determined by the evolution in CE after the primary leaves MS and engulfs its companion. Depending on details of this phase either merger of both components occurs (Tylenda *et al.* 2011, Stępień 2011b) or double degenerate star is formed (Brown *et al.* 2013).

Sections consecutively present observations and equipment used, method of light curve analysis, the resulting binary parameters and their discussion, then the evolutionary model of the variable, and finally the conclusions.

2. Observations and Data Reduction

2.1. Photometry

The photometric instrument included a 0.28-m Schmidt-Cassegrain telescope with an ST-8XME CCD camera mounted at the Cassegrain focus. Automated imaging was performed with photometric *B, V* and I_c filters manufactured to match the Bessell prescription. The computer clock was updated immediately prior to each session and exposure time for all images adjusted to 75 s. Details regarding image acquisition (lights, darks, and flats), calibration and registration can be found elsewhere (Alton 2016). Further photometric reduction to LCs was accomplished using four non-varying comparison stars (Table 1) in the same field-of-view (FOV). Since only data from images taken above 30° altitude (airmass < 2.0) were used, error due to differential refraction and color extinction was minimized and not corrected. Instrumental readings were reduced to MPOSC3 catalog-based magnitudes (Warner 2007).

T a b l e 1

Astrometric coordinates (J2000) and color indices $(B-V)$ for TYC 01664-0110-1 and four comparison stars used in this study

Star Identification	R.A.	Dec.	MPOSC3[a] $(B-V)$
TYC 01664-0110-1	$21^h29^m15\overset{s}{.}04$	$16°04'54\overset{''}{.}6$	0.970
TYC 01664-0500-1	$21^h29^m36\overset{s}{.}83$	$16°06'34\overset{''}{.}5$	1.272
2MASS 21293722+1605181	$21^h29^m37\overset{s}{.}22$	$16°05'18\overset{''}{.}2$	0.832
2MASS 21294091+1604521	$21^h29^m40\overset{s}{.}91$	$16°04'52\overset{''}{.}1$	1.224
2MASS 21293580+1604404	$21^h29^m35\overset{s}{.}80$	$16°04'40\overset{''}{.}4$	0.781

a: MPOSC3 is a hybrid catalog which includes a large subset of the Carlsberg Meridian Catalog (CMC-14) as well as from the Sloan Digital Sky Survey (SDSS).

2.2. Light Curve Analysis

Roche modeling was performed with Binary Maker 3 (BM3: Bradstreet and Steelman 2002), WDwint v5.6a[1], and PHOEBE 0.31a (Prša and Zwitter 2005), the latter two of which employ the Wilson-Devinney (W-D) code (Wilson and Devinney 1971, Wilson 1979). Renderings depicting the spatial arrangement of the

T a b l e 2

Times-of-minima for TYC 01664-0110-1 used to assess potential changes in orbital period using eclipse timing residuals (ETR)

Times-of-Minima (HJD–2 400 000)	± Error	UT Date Observation	Type	Ref.
52754.9340	–	25 Apr 2003	s	1
55407.5576	0.0001	30 Jul 2010	p[a]	2
56134.3443	0.0003	25 Jul 2012	s	3
56134.4846	0.0003	25 Jul 2012	p	3
56139.2950	0.0002	30 Jul 2012	p	3
56139.4378	0.0005	30 Jul 2012	s	3
56155.4242	0.0002	15 Aug 2012	p	3
56155.5665	0.0002	16 Aug 2012	s	3
56203.6702	0.0002	03 Oct 2012	s	4
57282.6014	0.0001	17 Sep 2015	s	This study
57283.5922	0.0001	18 Sep 2015	p	This study
57284.5838	0.0002	19 Sep 2015	s	This study
57289.5355	0.0002	24 Sep 2015	p	This study
57307.5025	0.0002	12 Oct 2015	s	This study

s = secondary, p = primary, a: identified as secondary minimum in Ref. 2 (1) Pilecki and Stępień (2012), (2) Demircan *et al.* (2011), (3) Terzioğlu *et al.* (2015), (4) Diethelm (2013).

[1]R.H. Nelson, 2009: *http://members.shaw.ca/bob.nelson/software1.htm*

binary stars in TYC 01664-0110-1 were generated by BM3 once model fits were finalized. The method of Kwee and van Woerden (1956) was used to calculate new times-of-minima (Table 2).

3. Results

3.1. Photometry and Ephemerides

The four comparison stars in the same FOV with TYC 01664-0110-1 showed little inherent variability beyond what would be expected from the equipment used and viewing location for this study. Over the period of image acquisition they stayed within ± 0.03 mag for V and I_c filters and ± 0.05 mag for B passband. Photometric values in B ($n = 259$), V ($n = 267$), and I_c ($n = 275$) were processed to generate three LCs that spanned 27 days between September 15 and October 12, 2015 (Fig. 1). In total, three new secondary (s) and two primary (p) minima were captured during this investigation. Data from all filters were averaged for each session (Table 2) since no color dependency on the timings was noted. After converting magnitude to flux, ROTSE-I, ASAS and UO light curve data (V-mag) were then folded together. The best fit was found where the orbital period

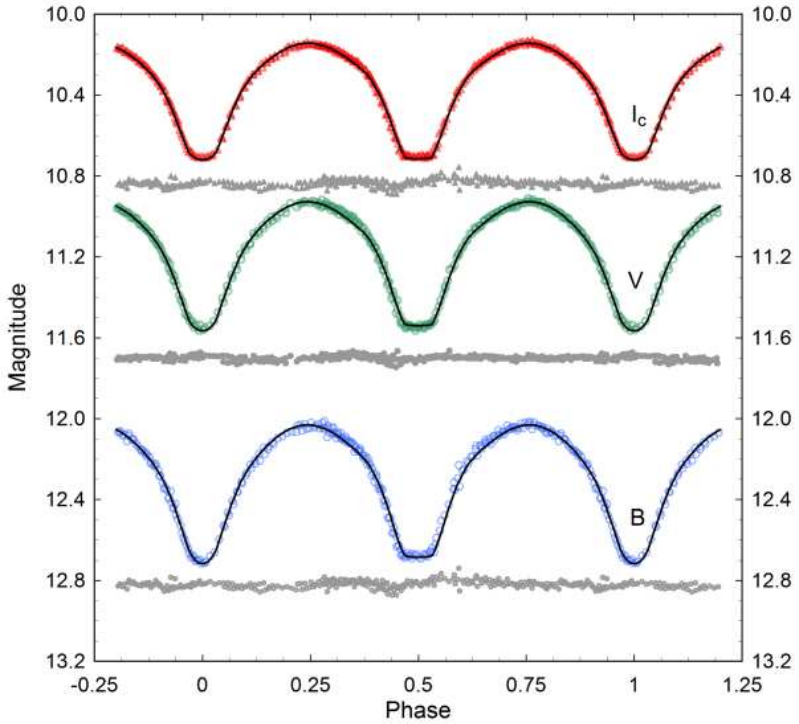

Fig. 1. Synthetic fits (solid-line) of TYC 01664-0110-1 light curves in B, V and I_c produced from CCD data collected at UO during 2015. The Roche model assumed an A-subtype W UMa binary with no spots. Residuals from the model fits are offset under each LC to keep the values on scale.

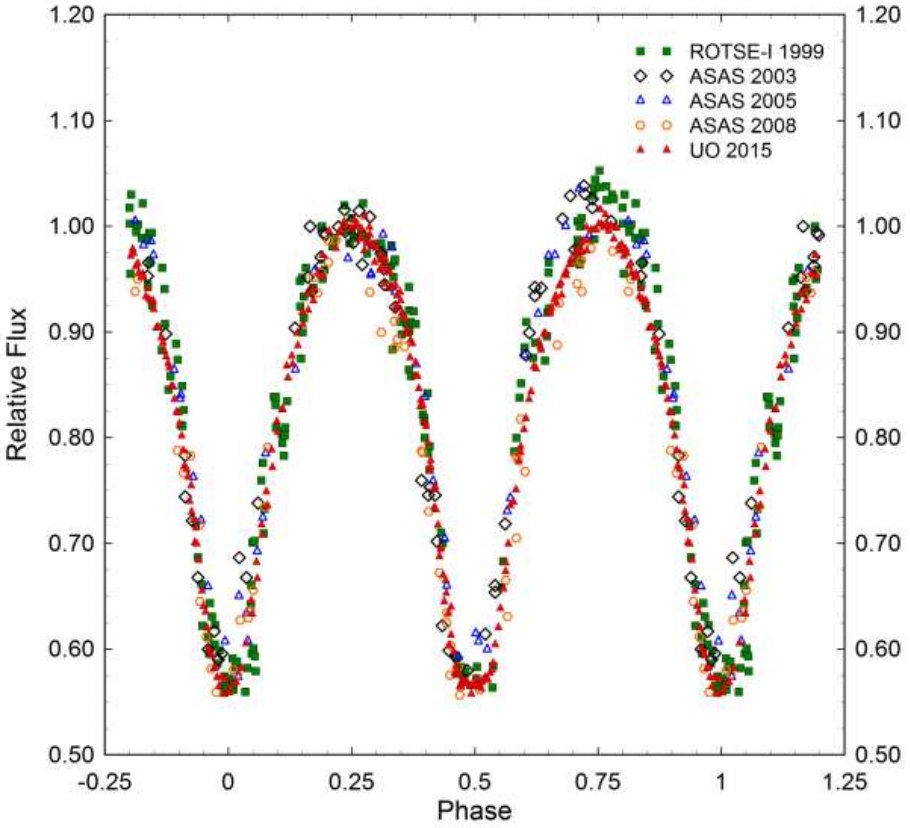

Fig. 2. Survey data from the ROTSE-I (1999), ASAS (2003–2008) and photometric results (*V*-mag) collected at UnderOak Observatory (2015) were folded together using period analysis ($P = 0.282960 \pm 0.000006$ d). Increased scatter at Max II ($\varphi \approx 0.75$) suggests the possibility of an active photosphere for TYC 01664-0110-1.

was 0.286960 ± 0.000006 d (Fig. 2). This was accomplished by applying periodic orthogonals (Schwarzenberg-Czerny 1996) to fit observations and analysis of variance (ANOVA) to evaluate fit quality (Vannmunster 2006)[2]. Fourier analysis (Harris *et al.* 1989) provided a similar period solution (0.2869609 ± 0.0000001) using only the multicolor data from UO.

A new linear ephemeris for the eclipse timings recorded between 2003 and 2015 was established with the following elements where:

$$\text{Min.I(hel)} = 2\,457\,307.3613(6) + 0.28296158(4)\,E. \qquad (1)$$

These data shown in Fig. 3 suggest that the orbital period of TYC 01664-0110-1 has remained fairly constant over the past 12 yr. This observation is in direct contrast to a positive period increase ($+0.059$ s/y) predicted by Lohr *et al.* (2015) with SuperWASP observations using a method described in an earlier publication (Lohr

[2]Peranso v2.5, Period Analysis Software. CBA Belgium Observatory

et al. 2014). It should be noted, however, that the corresponding reduced χ^2 value for a quadratic fit was poor in comparison to other systems which were investigated (see Table A.1 Lohr *et al.* 2015).

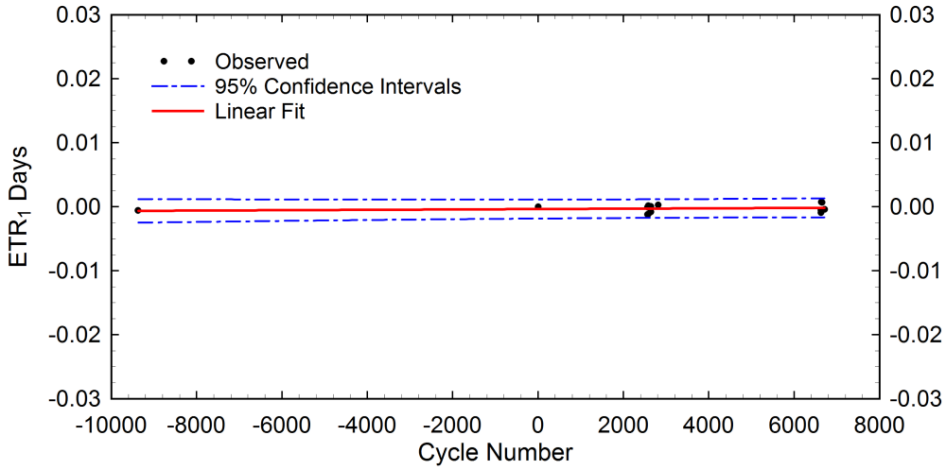

Fig. 3. Linear fit of eclipse timing residuals *vs.* epoch (25Apr2003 to 12Oct2015) illustrating no substantive change in orbital period for TYC 01664-0110-1.

3.2. Light Curve Behavior

Not unexpectedly, LCs (Fig. 1) from this W UMa binary system exhibit minima which are separated by 0.5 phase (φ) and consistent with a synchronous circular orbit. Notably, a flattened bottom at Min II implies that this binary system undergoes a total eclipse during which the larger star occults its smaller binary partner. Data from the ROTSE-I and ASAS surveys exhibit greater variability around Max II and to a lesser extent Min II (Fig. 2). A negative O'Connell effect (Max I fainter than Max II) is particularly noticeable in the photometric data collected during 1999, 2003 and 2005. This asymmetry has often been attributed to the presence of hot and/or cool starspot(s), impact from a gas stream, and/or other poorly understood phenomena which produce surface disturbances (Yakut and Eggleton 2005). The net result can be unequal heights during maximum light, often simulated by invoking starspot(s) during Roche-type modeling of the LC data.

3.3. Spectral Classification

Color index $(B-V)$ data from UO and five other surveys (Table 3) were corrected using the interstellar extinction ($A_V = 0.015$ mag, $E(B-V) = 0.005$ mag assuming $R = 3.1$) estimated for targets within the Galaxy according to the algorithm provided by Amores and Lépine (2005). A distance of 120 pc (see Section 3.6) was adopted for extinction calculations. The mean result, $(B-V)_0 = 0.964 \pm 0.041$ mag, which was adopted for subsequent Roche modeling indicates that the most luminous star in this system has an effective temperature of 4894 K

and ranges in spectral type between K2V and K3V (Pecaut and Mamajek 2013). For the sake of clarity, throughout this paper the larger more massive star is considered the primary irrespective of its effective temperature and it is denoted with the subscript "1" while subscript "2" denotes the secondary.

T a b l e 3

Spectral classification of TYC 01664-0110-1 based upon dereddened[a] $(B-V)$ data from various catalogs/surveys and the present study (UO)

Catalog/ Survey	$(B-V)_o$	$T_{\rm eff,1}^{\rm b}$	Spectral Class[c]
MPOSC3	0.97 ± 0.05	4877	K2V-K3V
2MASS	0.97 ± 0.15	4890	K2V-K3V
APASS	0.90 ± 0.03	5024	K2V-K3V
UCAC4	0.92 ± 0.02	4976	K2V-K3V
Terrell *et al.* (2012)	0.91 ± 0.18	5005	K2V-K3V
UO	1.12 ± 0.02	4530	K4V-K5V

a: $E(B-V) = 0.005$ mag, b: $T_{\rm eff}$ of the primary star interpolated and spectral class assigned from Pecaut and Mamajek (2013), c: Mean value for $(B-V)_0 = 0.964 \pm 0.041$ mag $T_{\rm eff,1} = 4894$ K, Spectral class = K2V-K3V.

3.4. Roche Modeling Approach

In the absence of *RV* data, it is not possible to unequivocally determine the mass ratio q or whether TYC 01664-0110-1 is an A- or W-type W UMa binary system. The short orbital period and a late spectral type are normally associated with the W-subtype. However, by definition, the deepest minimum (Min I) should occur when the hotter, but smaller star is occulted by the cooler more massive member of the binary system. Quite the opposite is found in that the flat-bottomed dip in brightness indicative of a total eclipse of the secondary occurs at Min II while the round-bottomed deeper minimum (Min I) results from a transit across the primary face. Consequently, we proceeded with W-D modeling under the assumption that this system is an A-type W UMa eclipsing binary. Roche modeling of LC data from TYC 01664-0110-1 was primarily accomplished using the program PHOEBE 0.31a (Prša and Zwitter 2005). The model selected was for an "overcontact binary not in thermal contact" (Mode 3) and each curve was weighted based upon observational scatter. Bolometric albedo ($A_{1,2} = 0.5$) and gravity darkening coefficients ($g_{1,2} = 0.32$) for cooler stars (< 7200 K) with convective envelopes were assigned according to Ruciński (1969) and Lucy (1967), respectively. The effective temperature of the more massive primary star was fixed ($T_1 = 4894$ K) according to the earlier designation as spectral type K2V to K3V. Following any change in the effective temperature for the secondary (T_2), new logarithmic limb

darkening coefficients (x_1, x_2, y_1, y_2) were interpolated according to Van Hamme (1993). All parameters except for T_1, $A_{1,2}$ and $g_{1,2}$ were allowed to vary during DC iterations. Roche modeling was initially seeded with $q = 0.35$ and $i = 88^\circ$ based upon parameters calculated for this system by Pilecki and Stępień (2012). Generally the secondary in an A-type has a lower effective temperature compared to the primary star but in this case a slightly higher ($\Delta T \approx 100$ K) value was required to achieve the best fit LC simulations. This assessment only included synthesis of light curves for TYC 01664-0110-1 without the incorporation of a spot since the so-called O'Connell effect at maximum light is barely evident in the 2015 LCs.

T a b l e 4

Synthetic light curve parameters employed for Roche modeling and the geometric elements determined when assuming that TYC 01664-0110-1 is an A-type W UMa variable

Parameter[a]	UO 2015, A-type no spot
T_1[a]	4894 K
T_2	4995 ± 5[b] K
q	0.356 ± 0.001[b]
A[a]	0.5
g[a]	0.32
$\Omega_1 = \Omega_2$	2.542 ± 0.003[b]
i	$88^o.88 \pm 0.16$[b]
$L_1/(L_1+L_2)_B$[c,d]	0.6818 ± 0.0002
$L_1/(L_1+L_2)_V$[c,d]	0.6920 ± 0.0001
$L_1/(L_1+L_2)_{Ic}$[c,d]	0.6985 ± 0.0001
r_1(pole)[c]	0.4510 ± 0.0005
r_1(side)[c]	0.4850 ± 0.0006
r_1(back)[c]	0.5143 ± 0.0007
r_2(pole)[c]	0.2830 ± 0.0013
r_2(side)[c]	0.2962 ± 0.0016
r_2(back)[c]	0.3362 ± 0.0030
Fill-out factor f	20.5%
$\chi^2(B)$[e]	0.001075
$\chi^2(V)$[e]	0.003828
$\chi^2(I_c)$[e]	0.007610

a: Fixed during DC, b: Error estimates for q, i, $\Omega_1 = \Omega_2$ and T_2 from heuristic scanning, c: Error estimates for spot parameters, $L_1/(L_1+L_2)$, r_1 and r_2 (pole, side and back) from WDwint v5.6a, d: Bandpass dependent fractional luminosity, L_1 and L_2 refer to luminosities of the primary and secondary stars, respectively, e: Monochromatic best Roche model fits (χ^2) from PHOEBE 0.31a (Prša and Zwitter 2005).

3.5. Light Curve Analysis

The initial estimates for q, i and T_2 quickly converged to a best fit Roche model solution (Table 4)[3]. Unspotted simulations (Fig. 1) revealed that contrary to expectations for an A-type W UMa binary, the effective temperature of the less massive secondary in this case is hotter than the primary. There is precedence in the literature for this phenomenon and has been observed with EK Com (Deb *et al.* 2010), HV Aqr (Gazeas *et al.* 2007), and BO CVn (Zola *et al.* 2012), all of which are LMCBs. A Roche surface outline model rendered with BM3 using the physical and geometric elements from the 2015 LCs is shown in Fig. 4. After a best model fit was found, values and errors for T_2, i, q and $\Omega_{1,2}$ were explored further using

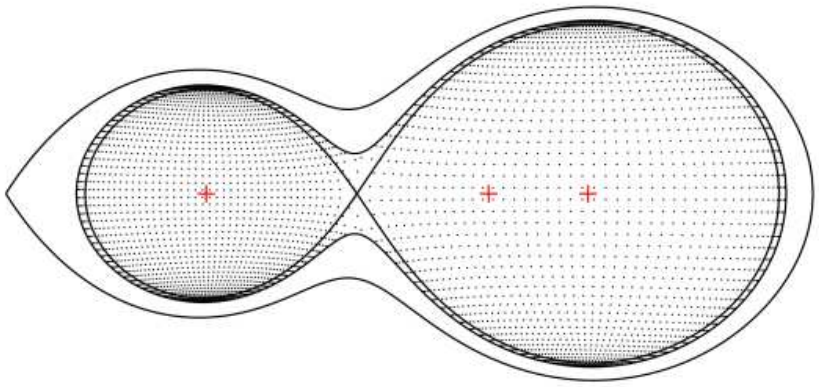

Fig. 4. Roche surface outline model of TYC 01664-0110-1 generated from 2015 photometric data.

the PHOEBE scripter where the W-D minimization program (DC) was repeatedly executed 1000 times (Prša and Zwitter 2005). During each heuristic scan, input parameter values are automatically updated for the next iteration. Thereafter, the formal error for each parameter was derived from the standard deviation observed with the outcome values. Binary systems which do not undergo a total eclipse suffer from degenerate solutions when simultaneously varying inclination i and mass ratio q during W-D modeling so that a reliable photometric determination of q is not possible (Terrell and Wilson 2005). In this case the light curves for TYC 01664-0110-1 clearly show the total eclipse of the secondary by the primary star at Min II. A probability contour ($\Delta\chi^2$) from the heuristic scan ($n = 1000$) of i *vs.* q (Fig. 5) illustrates that both parameters yield a unique fit within fairly narrow boundaries. The border which defines the 87% confidence interval ($\Delta\chi^2 = 4$) is consistent with a well-constrained value for $q = 0.356 \pm 0.003$ and $i = 88.^{\circ}90 \pm 0.^{\circ}85$. We should stress, however, that the listed errors result solely from a model fit to the observations, assuming exact values for all fixed parameters. In particular, the uncertainty of T_1, based on the calculated $(B-V)_0$, is not less than about 200–

[3]Errors reported in Tables 4, 5 and 6 are derived directly from fitting the Roche model and do not take into account all observational errors associated with these determinations.

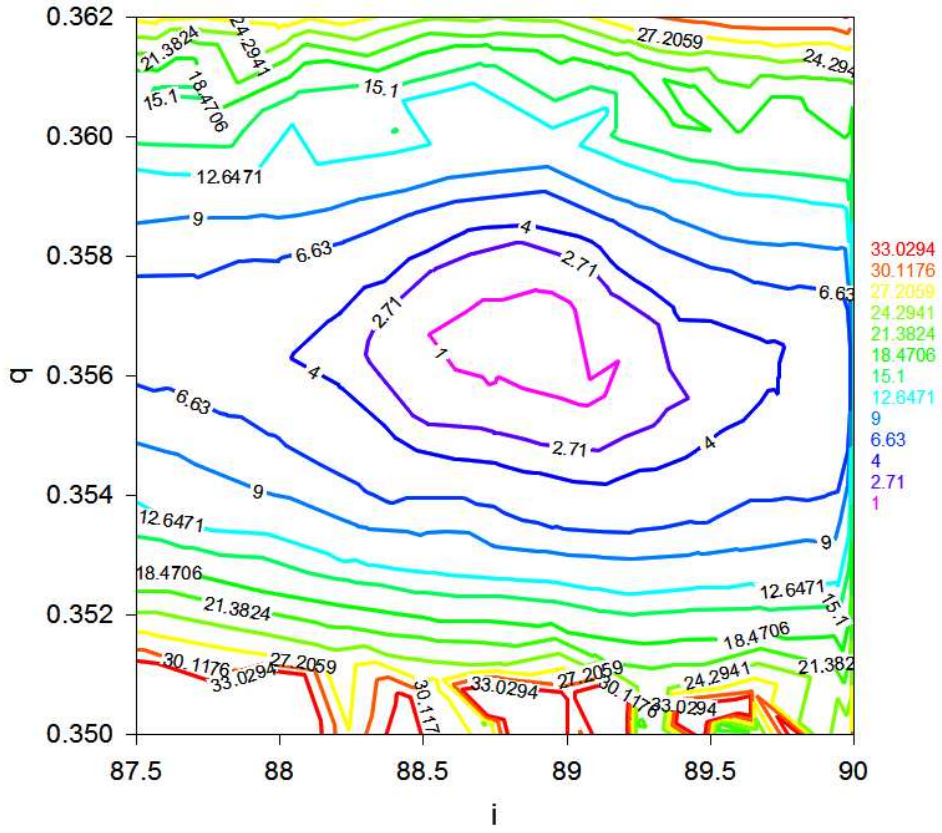

Fig. 5. Probability surface contour showing boundaries for a best fit when mass ratio q and the orbital inclination i are iteratively adjusted during DC. Randomized q and i values ($n = 1000$) were generated within $\pm 4\%$ of the nominal input values for q (0.356) and i (88.°88). The contours of $\Delta\chi^2 = \chi^2 - \chi^2_{\rm min}$ are shown. For a two-parameter fit true parameter values are within $\Delta\chi^2 = 4$ with $\approx 87\%$ confidence.

300 K if we take into account photometric errors, crude estimate of $E(B-V)$, calibration errors, etc. Varying T_1 by this amount would produce significantly larger (but also more realistic) errors.

The fill-out parameter f which is a measure of the degree-of-contact between each star was calculated according to Bradstreet (2005) where $\Omega_{\rm outer}$ is the outer critical Roche equipotential, $\Omega_{\rm inner}$ is the value for the inner critical Roche equipotential and $\Omega = \Omega_{1,2}$ denotes the common envelope surface potential for the binary system. The system is defined as a "contact binary" since the fill-out value (≈ 0.21) calculated for TYC 01664-0110-1 lies between $0 < f < 1$.

LMCB constituent stars typically are late spectral type (G-K) possessing low surface temperatures that are most likely magnetically active (Stępień and Gazeas 2012). Given this environment a large fraction of their surface may be covered with spots. A Roche model is needed which effectively addresses at least two phases ($\varphi = 0.50$ and $\varphi = 0.75$) of the LCs where obvious year-to-year changes are ob-

T a b l e 5

Comparison of synthetic light curve parameters employed for Roche modeling and the geometric elements determined when assuming that TYC 01664-0110-1 is an A-type W UMa variable

Parameter[a]	UO 2015 No spot *V*-flux	ROTSE-I 1999 Secondary Hot spot	ASAS 2003 Secondary Hot spot	ASAS 2005 Secondary Hot spot	ASAS 2008 Primary Cool spot
T_1[a]	4894 K	4894 K	4894 K	4894 K	4894 K
T_2[b]	4995 ± 5 K	4993 ± 13 K	5066 ± 17 K	4989 ± 22 K	5035 ± 22 K
q[b]	0.356 ± 0.002	0.337 ± 0.006	0.340 ± 0.012	0.339 ± 0.011	0.356 ± 0.011
A[a]	0.5	0.5	0.5	0.5	0.5
g[a]	0.32	0.32	0.32	0.32	0.32
$\Omega_1 = \Omega_2$	2.54 ± 0.01	2.52 ± 0.02	2.51 ± 0.03	2.51 ± 0.03	2.54 ± 0.03
i	88.88 ± 1.3[b]	88.88[a]	88.88[a]	88.88[a]	88.88[a]
$A_s = T_s/T$	–	1.11 ± 0.02	1.17 ± 0.03	1.15 ± 0.03	0.85 ± 0.08
Θ_s (spot co-latitude)[b,c]	–	65 ± 29	65 ± 8	65 ± 15	90 ± 6
ϕ_s (spot longitude)[b,c]	–	310 ± 15	310 ± 5	320 ± 7.6	$115. \pm 3$
r_s (angular radius)[b,c]	–	20 ± 1.7	16 ± 2	18.4 ± 2.1	10 ± 1.3
f (%)	20.5	12.6	20.0	21.7	20.5

a: fixed during DC, b: error estimates for q, i, $\Omega_1 = \Omega_2$, spot parameters and T_2 from WDwint v5.6, c: spot parameters Θ_s, ϕ_s and r_s are in degrees.

served (Fig. 6). The LCs observed in 1999, 2003 and 2005 are very similar in that Max II > Max I indicating a negative O'Connell effect. By contrast the 2008 LC exhibits a positive O'Connell effect (Max I > Max II). Inspection of these superimposed LCs (Fig. 2) reveals that when the flux is normalized to 1 at $\varphi = 0.25$, the relative intensity of light at Max I proves to be the least variable (0.998 ± 0.011) compared to those values observed at Min I (0.575 ± 0.012), Min II (0.577 ± 0.014) and Max II (1.009 ± 0.021). It follows that brightness at Max I and Min I varies the least which can also be said for their difference (0.423 ± 0.016). Normally it is not apparent whether the O'Connell effect results from an increase in light output during quadrature as might be expected from cool spot(s) on either star facing the observer or an elevation in brightness caused by a hot spot which is visible during maximum light. Since the flux between $\varphi = 0$ and $\varphi = 0.25$ stays relatively constant in all the LCs, arguably a case can be made that any attempt to model these data should focus on those parameters which primarily result in changes around Max II and to a lesser extent Min II. Initial fits were seeded with the final results (i, q, T_2 and $\Omega_{1,2}$) from the 2015 LCs. All other parameters ($A_{1,2}$, $g_{1,2}$ and T_1) remained fixed during DC. It became immediately apparent that due to the paucity of data around Min I and Min II that it was also necessary to fix the orbital inclination ($i = 88.^\circ 88$), otherwise very disparate solutions were obtained from the ROTSE-I and ASAS LCs. Depending on the light curve, a cool or hot spot was incorporated into the model to simulate peak asymmetry at maximum light. The ROTSE-I (1999) and ASAS (2003, 2005 and 2008) LCs are derived from sparse

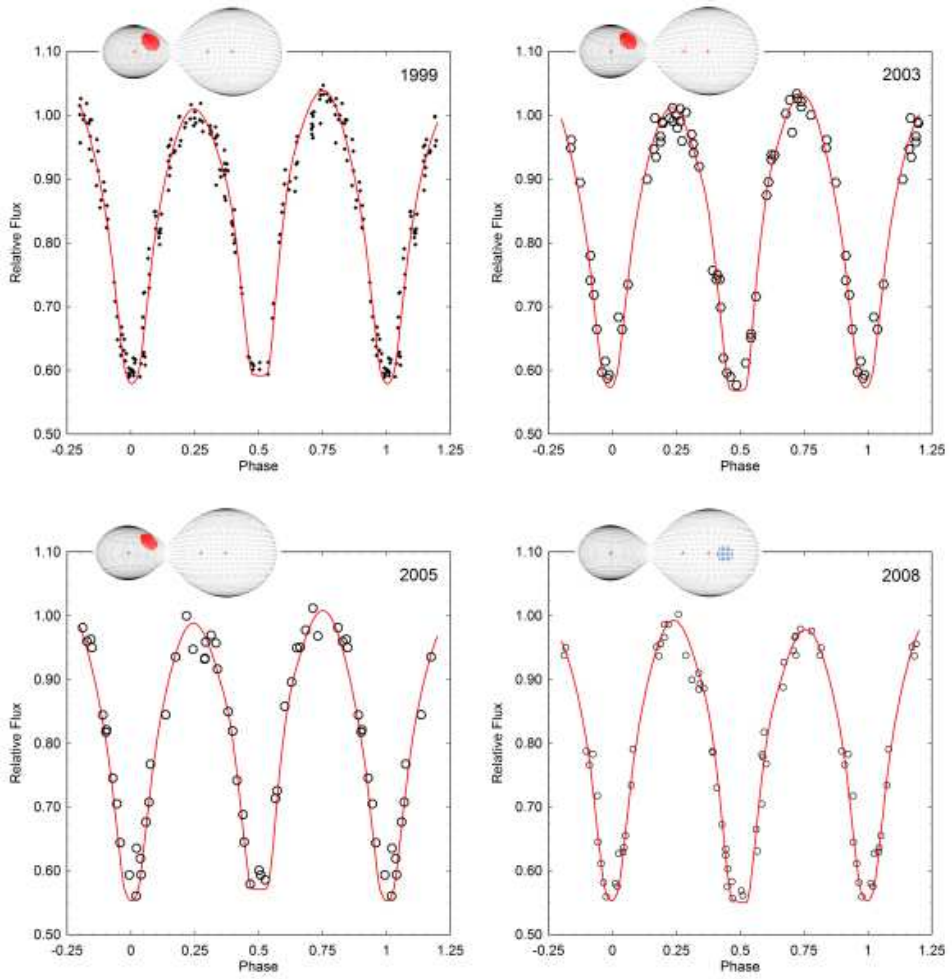

Fig. 6. LCs with corresponding Roche model fits (solid red line) and associated spatial representation with either a cool (blue) or hot (red) spot.

sampling over an eight month period during each year. Not surprisingly, Roche modeling produced more variable results compared to values derived from the UO 2015 LC (*V*-mag). The associated geometric and physical elements are summarized in Table 5 and the 3D-spatial models illustrated in Fig. 6. As expected, the Roche model solutions for the 1999, 2003 and 2005 LCs are very similar with only minor differences in T_2, the spot size and location. In all three instances, a hot spot on the less massive constituent provided the best overall LC simulations. The 2008 LC was best fit by positioning a cool spot on the primary star rather than on the side of the secondary facing the observer during Max II ($\varphi = 0.75$). Even though the associated LC minima are not data rich in 2003 and 2008, it would still appear that Min II is deeper than Min I, thus satisfying the definition for a W-type system. All the LCs presented herein offer a glimpse into the variable behavior of this binary system which may indicate deviations from the assumed Roche/Lucy model.

3.6. Absolute Parameter Estimates

Absolute parameters (Table 6) were derived for each star in this putative A-type W UMa binary system using results from the best fit simulation of the 2015 LCs. Total mass cannot be calculated directly without supporting *RV* data, however, estimates for stellar mass and radii from binary systems have been tabulated according to spectral type (Harmanec 1988). In this case, the primary star ($T_1 = 4894$ K) in TYC 01664-0110-1 is estimated to have a mass of 0.81 $M_\odot$ based on its K2-K3V classification. Alternatively, empirically determined period-mass relationships for W UMa-binaries have been established by Gazeas and Stępień (2008) and Qian (2003). Gazeas and Stępień (2008) found that the mass of the primary star (M_1) can be calculated from the following expression:

$$\log M_1 = (0.755 \pm 0.059) \log P + (0.416 \pm 0.024) \quad (2)$$

while the mass of the secondary (M_2) can be correspondingly estimated according to the following relationship:

$$\log M_2 = (0.352 \pm 0.166) \log P - (0.262 \pm 0.067). \quad (3)$$

T a b l e 6

Absolute parameters for TYC 01664-0110-1 using results from Roche modeling of the 2015 LCs

Parameter	Primary	Secondary
Mass [$M_\odot$]	0.92 ± 0.04	0.33 ± 0.01
Radius [$R_\odot$]	0.92 ± 0.01	0.57 ± 0.01
a [$R_\odot$]	1.95 ± 0.02	–
Luminosity [$L_\odot$]	0.434 ± 0.010	0.184 ± 0.004
$M_{\rm bol}$	5.66 ± 0.02	6.59 ± 0.02
$\log g$	4.47 ± 0.02	4.44 ± 0.01

The results indicate that $M_1 = 1.01 \pm 0.09$ $M_\odot$ for the primary and $M_2 = 0.35 \pm 0.09$ $M_\odot$ for the secondary star. The value for the photometrically determined mass ratio ($q_{ph} = 0.356 \pm 0.001$) from this study is within the mass ratio and error ($q = 0.349 \pm 0.095$) calculated according to Gazeas and Stępień (2008). Qian (2003) derived another mass-period relationship

$$\log M_1 = (0.761 \pm 0.150) \log P + (1.82 \pm 0.28) \quad (4)$$

for contact binaries when $M_1 < 1.35$ $M_\odot$ and $P < 0.41$ d. In this case the solution leads to a somewhat lower estimate for the mass ($M_1 = 0.946 \pm 0.076$ $M_\odot$) of

the primary star. For the purposes of this study, the average of all three values ($M_1 = 0.92 \pm 0.04$ M$_\odot$) was used for subsequent determinations of M_2, semi-major axis a, volume-radius r_L, bolometric magnitude $M_{\rm bol}$ and distance d [pc] to TYC 01664-0110-1. The semi-major axis, $a = 1.95 \pm 0.02$ R$_\odot$, was calculated according to Kepler's third law. Using the expression derived by Eggleton (1983) volume radius values were determined for the primary ($r_1 = 0.4703 \pm 0.0003$) and secondary ($r_2 = 0.2940 \pm 0.0002$) stars. Absolute radii for both binary constituents were calculated where $R_1 = a \times r_1 = 0.918 \pm 0.010$ R$_\odot$ and $R_2 = a \times r_2 = 0.574 \pm 0.006$ R$_\odot$. We neglect here that both stars protrude somewhat above their inner Roche lobes. Assuming that $T_1 = 4894$ K, $T_2 = 4995$ K and $T_\odot = 5778$ K, then the bolometric magnitudes are $M_{\rm bol,1} = 5.66 \pm 0.024$ mag and $M_{\rm bol,2} = 6.59 \pm 0.024$ mag while the luminosities for the primary and secondary are $L_1 = 0.434 \pm 0.010$ L$_\odot$ and $L_2 = 0.184 \pm 0.004$ L$_\odot$, respectively. The combined bolometric magnitude for this binary system was calculated to be $M_{\rm bol,tot} = 5.27 \pm 0.026$ mag.

The distance to TYC 01664-0110-1 was estimated (113 ± 1 pc) using the distance modulus equation corrected for interstellar extinction A_V. In this case *V*-mag at maximum light ($m = 10.93 \pm 0.01$ mag) is adopted, and $M_V = M_{\rm bol,tot} - BC = 5.65 \pm 0.03$ mag is the *V* absolute magnitude. Here $BC = -0.372$ mag is the bolometric correction (Pecault and Mamajek 2013) and $A_V = 0.015$ mag the interstellar extinction which was determined in Section 3.3. A second estimate for distance to this system was performed after calculating the absolute bolometric magnitude (M_V) according to the empirical relationship defined by Rucinski and Duerbeck (1997):

$$M_V = -4.44 \log P + 3.02 (B-V)_0 + 0.12. \quad (5)$$

Substituting $m = 10.93 \pm 0.01$ mag, the newly determined value for M_V (5.47 ± 0.12) mag and A_V (0.015 mag) back into the distance modulus equation produced an estimate of 123 ± 7 pc. A third value (125 ± 14 pc) was calculated according to the empirical expression derived by Gettel *et al.* (2006) from a ROTSE-I catalog of W UMa binary stars:

$$\log d = 0.2m - 0.18 \log P - 1.6(J-H) + 0.56 \quad (6)$$

where again $m = 10.93 \pm 0.01$ mag and $(J-H)$ is taken from the 2MASS catalog. The combined mean distance places this system about 121 ± 5 pc away.

4. Evolutionary Model of the Binary

4.1. Model Description

The search for a progenitor of the investigated binary is based on a model developed by one of us (Stępień 2006, Gazeas and Stępień 2008, Stępień and Kiraga 2015). It describes the evolution of a cool close binary from the zero-age main sequence (ZAMS) until a stage preceding the merger of the components or formation of a common envelope (CE).

The basic equations of the model are the third Kepler law, the approximate expressions for inner Roche-lobe sizes and the standard expression for binary angular momentum (see *e.g.*, Stępień and Kiraga 2015).

It is assumed that both components rotate synchronously with the orbital period and possess subphotospheric convection layers causing the magnetic activity. As such, magnetized winds from the two components and the mass transfer between them, are the dominating mechanisms of the orbit evolution. The winds carry away mass and angular momentum (AM) according to the formulae

$$\dot{M}_{1,2} = -10^{-11} R_{1,2}^2, \tag{7}$$

$$\frac{\mathrm{d}H_{\mathrm{tot}}}{\mathrm{d}t} = -4.9 \times 10^{41} (R_1^2 M_1 + R_2^2 M_2)/P. \tag{8}$$

Here H_{tot} is the total (orbital and rotational) AM in cgs units, $\dot{M}$ is in solar masses per year and $\mathrm{d}H_{\mathrm{tot}}/\mathrm{d}t$ is in g cm^2/s per year. The formulae are calibrated by the observational data of the rotation from single, magnetically active stars of different age, and empirically determined mass-loss rates of single, solar types stars. Both formulae apply in a limiting case of a rapidly rotating star in the saturated regime when magnetic activity is at a maximum. Note that they do not contain any free adjustable parameters. The constant in Eq.(7) is uncertain within a factor of 2 and that in Eq.(8) is uncertain to $\pm$30% (Stępień 2006). The model ignores any interaction between winds from the two components.

The evolutionary calculations are divided into three phases: from ZAMS to the Roche lobe overflow (RLOF) by the initially more massive component (henceforth donor), rapid, conservative mass exchange from the more to less massive component (henceforth accretor), and the third phase of a slow mass exchange resulting from nuclear evolution of the donor. Single star evolutionary models PARSEC (Bressan *et al.* 2012), supplemented by the models of very low mass stars, calculated far beyond MS by Dr. Ryszard Sienkiewicz, (see Stępień 2006) are used to approximate the evolution of both components at each time step. Note that after the rapid mass transfer phase the accretor becomes the more massive component and thereby corresponds to the presently observed primary.

4.2. Results of the Model Computations

The initial donor and accretor masses ($M_{\mathrm{d,i}}$ and $M_{\mathrm{a,i}}$, respectively) in solar units together with the initial orbital period P_{i} in days fully describe the initial model. We denote each model by the combination: $M_{\mathrm{d,i}} + M_{\mathrm{a,i}}(P_{\mathrm{i}})$, *e.g.*, 1.03+0.34 (3.375). Starting with the initial parameters, Eqs.(7–8) are integrated, component masses and AM computed at each time step and all other stellar parameters (radii, temperatures and luminosities) interpolated from the PARSEC grid. When the size of the accretor exceeds its Roche lobe, rapid mass transfer takes place (here assumed at the constant rate of $5 \times 10^{-9}\,\mathrm{M}_{\odot}$/yr so that a half solar mass is transferred

in 10^8 years). Values of stellar parameters are not correctly described during this phase because in reality both components are out of thermal equilibrium. Nonetheless, this phase always takes a very short time compared to the evolutionary time scale and, as long as the process is conservative, its ultimate outcome is uniquely determined when the accretor dives below its Roche lobe and both stars regain equilibrium. In the third phase the donor expands at the evolutionary time scale and transfers mass to the accretor at the rate proportional to the excess of the donor's size above the Roche lobe. During all evolutionary phases AML takes place according to Eq. (8), *i.e.*, at the rate inversely proportional to the period length. Mass transfer and AML influence the orbital period in opposite directions and their balance specifies whether the period increases or decreases.

A unique progenitor of a given binary can be determined (within the adopted evolutionary model) only if the binary age is known in addition to basic parameters, like masses, radii, temperatures, orbital period and metallicity. Otherwise a number of possible progenitors can be found with different ages and different evolutionary histories (Stępień 2011b). The age of TYC 01664-0110-1 is unknown but, fortunately, the present values of its parameters severely restrict a possible range of acceptable progenitors. Given its mass, the oversized donor radius indicates that the star possesses a small helium core (see Fig. 1 in Stępień 2006) which means that its initial mass must have been high enough to have already left the MS. A coarse search in the initial parameter space showed that the initial donor mass must exceed 1 $M_\odot$ assuming the solar metallicity ($Z = 0.014$). A donor mass automatically determines the accretor mass because the total initial binary mass must be equal to the present mass plus the amount lost by the winds. On the whole we have $M_{\rm tot,i} \approx 1.35 M_\odot$.

After a refined search in the initial parameter space we found two models with donor mass close to the minimum mass, which satisfactorily reproduce the present parameters of TYC 01664-0110-1. Table 7 lists the relevant data and compares them with observations.

T a b l e 7

Comparison of the observed parameters of binary TYC 01664-0110-1 with the two best fitting models

Name/Parameter	P [d]	a [$R_\odot$]	$M_{\rm a}$ [$M_\odot$]	$M_{\rm d}$ [$M_\odot$]	$R_{\rm a}$ [$R_\odot$]	$R_{\rm d}$ [$R_\odot$]	$L_{\rm tot}$ [$L_\odot$]	T_e
TYC 01664-0110-1	0.283	1.95	0.92	0.33	0.92	0.57	0.618	4943
1.03+0.34(3.375)	0.283	1.956	0.919	0.331	0.815	0.584	0.664	5224
1.05+0.30(3.59)	0.283	1.949	0.916	0.330	0.810	0.582	0.649	5212

Subscripts "a" and "d" correspond to the present primary and secondary, respectively

As can be seen from Table 7, the initial mass ratio of either progenitor is quite large, $q_{\rm i} = 3{-}3.5$, where $q_{\rm i} = M_{\rm d,i}/M_{\rm a,i}$ (the initial donor and accretor masses are given in the first column of Table 7). The minimum period during the rapid mass exchange reaches 0.224 and 0.182 d for the first and second model from Table 7, respectively, which is long enough that the process is conservative, particularly if it takes place in the form of an equatorial stream described by Stępień and Kiraga (2013). This should prevent the donor from excessive inflation following loss of thermal equilibrium. Nevertheless, the larger the initial mass ratio is, the higher the probability of losing a significant fraction of mass during the rapid mass exchange phase. Therefore, we did not consider models with mass ratios exceeding 3.5.

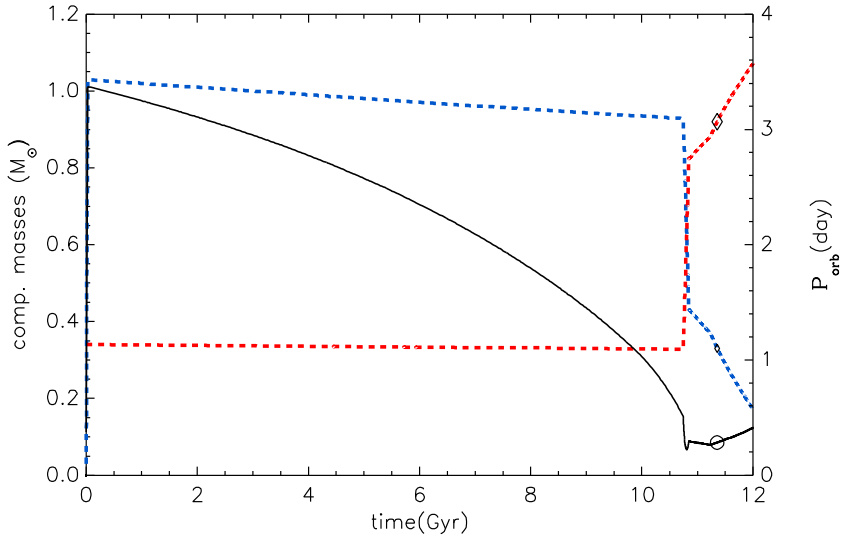

Fig. 7. Time evolution of component masses (broken lines: blue – donor, red – accretor) and orbital period (solid line) of the model 1.03+0.34(3.375). Observed masses are shown as diamonds with sizes approximately reflecting the estimated errors. The observed value of the orbital period is shown as an open circle.

Fig. 7 shows time variations of component masses and orbital period for the model 1.03+0.34(3.375). The analogous figure for the model 1.05+0.30(3.59) looks very similar. The present values of the binary parameters are best reproduced when the model 1.03+0.34(3.375) reaches the age of 11.354 Gyr. The corresponding age for the other model is 9.963 Gyr. The advanced age of about 10 Gyr suggests that TYC 01664-0110-1 is an old disk star. This is in agreement with the results of Bilir *et al.* (2005) who found an age of 9 Gyr for the group of W UMa stars with periods shorter than 0.3 d. The star has a sizeable Galactic latitude of about 25° indicating that it populates the thick disk. The period of the fitting model increases presently at the rate $\mathrm{d}P/\mathrm{d}t = 1.5 \times 10^{-5}$ s/yr due to the mass transfer of about $3 \times 10^{-10}\mathrm{M}_{\odot}$/yr. This is far beyond the present capabilities of detection.

If evolution continues according to our model, after an additional 4.3×10^{8} yr the donor will reach a mass of 0.2 $\mathrm{M}_{\odot}$ at which time the orbital period will have

increased to 0.36 d. Even later evolutionary stages are not correctly described by the present model so we can only speculate about the ultimate fate of the binary. Most likely, a CE develops at some point due to the evolutionary expansion of the accretor. This is a different outcome from the majority of LMCBs which finish their evolution by merging together when the components are still on the MS (Stępień and Gazeas 2012). The reason seems to lie in a large initial mass ratio. Detached binaries with the total mass low enough to form an LMCB will reach contact configuration for a broad range of mass ratios: $1 \leq q_{\rm i} \leq 3-3.5$ if the initial period is sufficiently short for RLOF to occur within the age of the Universe (Stępień and Gazeas 2012). Longer period binaries have remained detached and are part of the present day observational record. Binaries from a narrow $q_{\rm i}$ ranging between 3–3.5 and periods around 3.5 d can form LMCBs with periods slowly increasing and mass ratio decreasing in the third evolutionary phase. As a result, binaries similar to TYC 01664-0110-1 or OU Ser (Zola *et al.* 2005) are formed. Binaries with still larger mass ratios will certainly lose a substantial fraction of mass and AM following RLOF and quickly merge together.

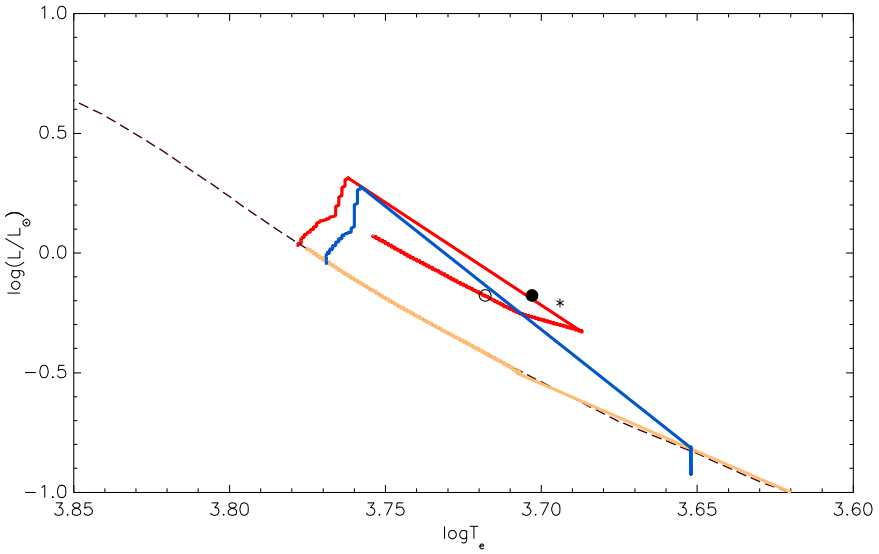

Fig. 8. Evolutionary track of the model 1.03+0.34(3.375) on the HR diagram. The PARSEC isochrone (10^8 yr) for $Z = 0.015$, approximating ZAMS, is shown with long brown dashes. The accretor track which closely follows ZAMS is shown with a yellow line, the donor track with a blue line and the track for the whole binary as a red line. The presently observed position of TYC 01664-0110-1 is shown with an asterisk, open circle shows the model data listed in Table 7 whereas the filled circle shows the data of the radius corrected model (see text).

Evolution of the model 1.3+0.34(3.375) in the HR diagram is shown in Fig. 8. Here lines corresponding to the evolution of the accretor (yellow line), donor (blue line), and red line (whole binary) are plotted together with an isochrone of 10^8 years (brown dotted line) which mimics ZAMS. The accretor evolves upward,

closely to ZAMS. During the first, detached phase of the binary evolution a $0.34\,M_\odot$ star negligibly moves away from ZAMS. During the rapid mass exchange and later it is fed with hydrogen rich matter from its companion, so it continues to stay closely to ZAMS. The donor, on the contrary, moves away from ZAMS during the detached phase until it fills its Roche lobe, loses a substantial fraction of its mass following RLOF, moves downward on the HR diagram and continues this route in the third phase of slow mass transfer. An asterisk shows the present temperature and luminosity of TYC 01664-0110-1 whereas an open circle gives the same data for the model 1.3+0.34(3.375) at the age of 11.354 Gyr. Note that the radius of the accretor is significantly smaller at this age than the radius of its observed counterpart (see Table 7). In fact, it is even a little lower than the size of the Roche lobe. Neglecting all effects resulting from lack of thermal equilibrium, proximity and the high level of activity is the most probable reason for this discrepancy. Active cool stars show systematically larger radii by up to 10% than resulting from the models (Torres *et al*. 2010). If we inflate the accretor by 10%, its temperature will drop correspondingly and so will the total binary temperature. The filled circle gives the result. As we see, the agreement between the observations and the radius-corrected model is now remarkably good.

4.3. Discussion

How robust is our modeling of TYC 01664-0110-1? Uncertainties of the evolutionary modeling procedure outlined in Section 4.1 are discussed in detail by Stępień and Kiraga (2015). Here we only mention that the main sources of uncertainties are connected with uncertainties of the coefficients in Eqs. (7–8), unknown metallicity of TYC 01664-0110-1, neglected here influence of magnetic activity on stellar parameters and uncertainties connected with the use of a particular set of single star models. Altogether, we estimate the total uncertainty of the progenitor parameters at about 10%.

Equal- or almost equal-depth minima observed in W UMa-type stars require the average surface brightness to be uniform over the common stellar surface and that in turn involves a substantial energy transfer from primary to secondary or, in the model nomenclature, from accretor to donor (Mochnacki 1981). This takes place most likely *via* a large-scale mass stream flowing from accretor, encircling the donor along the equatorial strip and returning to its parent star (Stępień 2009). In binaries with poor thermal contact the low efficiency of energy transfer renders the massive component significantly hotter than its low mass component whereas a deep thermal contact makes transfer very efficient which results in equal (or almost equal) surface averaged temperatures. In other words, the energy transfer between the presently more massive component (accretor) and its less massive component (donor) requires that $\Delta T = T_\mathrm{a} - T_\mathrm{d} \geq 0$. Yet, a negative difference is observed in many W UMa stars. Obviously, the surface layers of the accretor cannot be genuinely cooler than those of the donor – energy transfer from cool to hot medium vio-

lates basic laws of physics. So, the most viable explanation of this paradox assumes the presence of cool, heavily spotted areas on the massive component (Rucinski 1993). The unperturbed photospheric temperature is still higher than that of the donor but the surface averaged temperature may be lower. The W-phenomenon (negative ΔT) is, indeed, observed only in binaries with primaries less massive than about 1.5 $M_\odot$ which are expected to show high level of activity, contrary to more massive primaries. A moderate spot coverage of about 25% can be responsible for $\Delta T \approx -170$ K and when it approaches 50% the temperature difference can be (algebraically) lower than -500 K (Stępień 2009). The amount of transferred energy can be estimated from a comparison of the core energy of each component with the surface radiated energy. The data for the model 1.03+0.34(3.375) resulting from the core energy are as follows: $T_{\rm a} = 5495$ K, $L_{\rm a} = 0.541$, $T_{\rm d} = 4487$ K and $L_{\rm d} = 0.122$. To estimate the amount of transferred energy let us assume constant temperature averaged over the common stellar surface of the model. We obtain 5244 K so the energy radiated by the accretor and donor is equal to 0.442 $L_\odot$ and 0.222 $L_\odot$, respectively. The model temperature is higher than the observed one due to the lower accretor radius compared to the primary component radius (Table 7). From the comparison with the core energy we see that about 0.1 $L_\odot$ energy is constantly transferred from the accretor to the donor. This amount of energy indicates that the stream encircling the donor covers between 2/3 and 3/4 of its surface (see Fig. 7 in Stępień 2009).

Light curves of W UMa stars show sometimes another feature, poorly described by the W-D model. This is the O'Connell effect. More prominent O'Connell effect occurs usually when Max I is brighter than Max II (positive effect) and can reach $0\overset{\rm m}{.}1$ (Pilecki 2010). An even larger asymmetry in height during maximum light is visible with near-contact binaries, *e.g.*, in V361 Lyr (Hilditch *et al.* 1997) or in binaries presumably in contact with a particularly large difference between the component temperatures (Siwak *et al.* 2010). To reproduce this effect in simulated light curves, a bright spot is placed on the trailing face of the low mass component. Its origin is most likely connected with the stream of hot matter interacting with the surface of a cooler star and forming an equatorial bulge (Stępień 2009). In binaries with a poor thermal contact (signified by minima of different depth) the feeble stream cools down before it returns to the hot component and the O'Connell effect is clearly visible. In binaries with a very good thermal contact it is barely visible as the cooling of the massive stream encircling the cool component is very limited. In such variables a variable spottiness on the primary may even produce a small negative O'Connell effect. TYC 01664-0110-1 is a good example of such a situation. Strongly variable spottiness, observed in many W UMa stars (Pilecki 2010) may also be responsible for a transition from W- to A-type contact binary and *vice versa*. All these features indicate a dynamical character of the processes taking place in cool contact binaries, which are not correctly described by the commonly used W-D model (Rucinski 2015).

5. Conclusions

Five new times-of-minima for the W UMa binary system TYC 01664-0110-1 were captured in *B*, *V* and I_c passbands using a CCD camera. A revised linear ephemeris that includes all available times-of-minima suggests that the orbital period of TYC 01664-0110-1 has remained fairly constant over the past twelve years. This is a relatively short period of time such that many more years of data will need to be collected in order to determine whether there are any secular changes in orbital period. Findings from this study and other surveys suggested that the effective temperature of the most luminous star is 4894 K which corresponds to K2V-K3V spectral class. Uncommonly, the less massive secondary in this putative A-type W UMa binary is somewhat hotter ($\Delta T \approx 100$ K) than its primary partner. This phenomenon has been reported with other A-type systems especially EK Com (Deb *et al.* 2010) which is strikingly similar in size and luminosity to TYC 01664-0110-1. Without *RV* data it is not possible to unequivocally determine a mass ratio (q). Nonetheless this system undergoes a clearly defined total eclipse at Min II which is evident as a flat-bottomed dip in brightness. As such, a photometric solution for mass ratio is well constrained during DC optimization of LC data within the W-D code. This value ($q = 0.356$) is nearly identical to that reported by Pilecki and Stępień (2012) and is expected to correlate well with a spectroscopically derived mass ratio. Nonetheless, until *RV* data become publicly available, these Roche model fits and any absolute parameters derived for this W UMa binary are subject to greater uncertainty. Since maximum light at $\varphi = 0.25$ and 0.75 was nearly equal in the 2015 LCs, a spotted solution did not significantly improve the fits to the Roche model. This is in contrast to LCs collected in 1999, 2003, 2005 and 2008 from the ROTSE-I and ASAS surveys which exhibit notable peak asymmetry suggesting that this system has an active photosphere. Roche modeling of these sparsely sampled LCs revealed that the unequal brightness observed during quadrature can be simulated with the addition of a single hot spot (1999, 2003 and 2005) on the secondary star or by positioning a cool spot on the primary (2008).

The binary is an exceptional object in the sense that it has a short orbital period, shows total eclipses and is quite bright ($m_{V,\max} \approx 10.9$ mag). It seems to be an excellent target for the detailed comparison of the dynamical processes taking place in a short period W UMa-type star with the results obtained by Rucinski (2015) for AW UMa. High quality spectra with short time exposures are necessary for such an analysis.

Based on the evolutionary model of cool close binaries, possible progenitors of TYC 01664-0110-1 were searched. The results show that a close binary with the initial orbital period of about 3.5 d and component masses of 1.0–1.1 $M_\odot$ and 0.30–0.35 $M_\odot$ is the most probable progenitor of this variable. A period with this value lies close to the local maximum of the period distribution produced by a mechanism called Kozai cycles with tidal friction (Fabrycky and Tremaine 2007, Naoz and Fabrycky 2014). The present parameters of TYC 01664-0110-1 are reproduced by

the model at the age of about 10 Gyr. This indicates that TYC 01664-0110-1 is an old disk star. A narrow range of the permissible initial parameters results in a rare LMCB which, according to our model, will not merge due to the rapid decrease of the period, as most other LMCBs will do (Stępień and Gazeas 2012) but, instead, it will very likely go through a CE phase ultimately merging or forming a short period double degenerate.

Acknowledgements. This research has made use of the SIMBAD database, operated at Centre de Données astronomiques de Strasbourg, France, the Northern Sky Variability Survey hosted by the Los Alamos National Laboratory, the All Sky Automated Survey (ASAS) and the International Variable Star Index maintained by the AAVSO. The diligence and dedication shown by all associated with these organizations is very much appreciated.

REFERENCES

Alton, K.B. 2016, *JAAVSO*, in press.
Amores, E.B., and Lépine, J.R.D. 2005, *AJ*, **130**, 659.
Bilir, S., Karataş, Y., Demircan, and O., and Eker, Z. 2005, *MNRAS*, **357**, 497.
Binnendijk, L. 1970, *Vistas in Astronomy*, **12**, 217.
Bressan, A., Marigio, P., Girardi, L.,Salasnich, B., Dal Cero, C., Rubele, S., and Nanni, A. 2012, *MNRAS*, **427**, 127.
Bradstreet, D.H. 2005, *The Society for Astronomical Sciences 24th Annual Symposium on Telescope Science*, 23.
Bradstreet, D.H., and Steelman, D.P. 2002, *BAAS*, **34**, 1224.
Brown, W.R., Kilic, M., Prieto, C.A., Gianninas, A., and Kenyon, S.J. 2013, *ApJ*, **769**, 66.
Deb, S., Singh, H.P., Seshadri, T.R., and Gupta, R. 2010, *New Astronomy*, **15**, 662.
Demircan, Y., *et al.* 2011, *IBVS*, 5965.
Diethelm, R. 2013, *IBVS*, 6042.
Eggleton, P.P. 1983, *ApJ*, **268**, 368.
Fabrycky, D., and Tremaine, S. 2007, *ApJ*, **669**, 1298.
Gazeas, K.D., Niarchos, P.G., and Zola, S. 2007, *ASP Conference Series*, **370**, 279.
Gazeas, K., and Stępień, K. 2008, *MNRAS*, **390**, 1577.
Gettel, S.J., Geske, M.T., and McKay, T.A. 2006, *AJ*, **131**, 621.
Harmanec, P. 1988, *Astronomical Institutes of Czechoslovakia, Bulletin*, **39**, 329.
Harris, A.W., *et al.* 1989, *Icarus*, **77**, 171.
Hilditch, R.W., Collier Cameron, A., Hill, G., Bell, A.A., and Harries, T.J. 1997, *MNRAS*, **291**, 749.
Hoffman, D.J., Harrison, T.E., and McNamara, B.J. 2009, *AJ*, **138**, 466.
Kwee, K.K., and Woerden, H. van 1956, *Bulletin of the Astronomical Institutes of the Netherlands*, **12**, 327.
Lohr, M.E., *et al.* 2014, *A&A*, **566**, A128.
Lohr, M.E., Norton, A.J., Payne, S.G., West, R.G., and Wheatley, P.J. 2015, *A&A*, **578**, A136.
Lucy, L.B. 1967, *Zeitschrift für Astrophysik*, **65**, 89.
Mochnacki, S. 1981, *ApJ*, **245**, 650.
Naoz, S., and Fabrycky, D.C. 2014, *ApJ*, **793**, 137.
Pecaut, M.J., and Mamajek, E.E. 2013, *ApJS*, **208**, 9.
Pilecki, B. 2010, PhD Thesis, Warsaw University.
Pilecki, B., and Stępień, K. 2012, *IBVS*, 6012.
Pojmański, G., Pilecki, B., and Szczygieł, D. 2005, *Acta Astron.*, **55**, 275.

Prša, A., and Zwitter, T. 2005, *ApJ*, **628**, 426.
Qian, S. 2003, *MNRAS*, **342**, 1260.
Ruciński, S. M. 1969, *Acta Astron.*, **19**, 245.
Rucinski, S. M. 1993, in: "The Realm of Interacting Binary Stars", Eds. J. Sahade, *et al.* Kluwer, Dordrecht, p. 111.
Rucinski, S.M. 2015, *AJ*, **149**, 49.
Rucinski, S.M., and Duerbeck, H. 1997, *PASP*, **109**, 1340.
Schwarzenberg-Czerny, A. 1996, *ApJ*, **460**, L107.
Siwak, M., Zola, S., and Koziel-Wierzbowska, D. 2010, *Acta Astron.*, **60**, 305.
Stępień, K. 2006, *Acta Astron.*, **56**, 199.
Stępień, K. 2009, *MNRAS*, **397**, 857.
Stępień, K. 2011a, *Acta Astron.*, **61**, 139.
Stępień, K. 2011b, *A&A*, **531**, A18.
Stępień, K., and Gazeas, K. 2012, *Acta Astron.*, **62**, 153.
Stępień, K., and Kiraga, M. 2013, *Acta Astron.*, **63**, 239.
Stępień, K., and Kiraga, M. 2015, *A&A*, **577**, 117.
Terrell, D., and Wilson, R.E. 2005, *Astrophys., and Space Sci.*, **296**, 221.
Terrell, D., Gross, J., and Cooney, W.P. Jr. 2012, *AJ*, **143**, 99.
Terzioĝlu, Z., *et al.* 2015, *IBVS*, , 6128.
Torres, G., Andersen, J., and Giménez, A. 2010, *Astronomy and Astrophysics Review*, **18**, 67.
Tylenda, R., *et al.* 2011, *A&A*, **528**, A114.
Van Hamme, W. 1993, *AJ*, **106**, 2096.
Warner, B. 2007, *The Minor Planet Bulletin*, **34**, 113.
Wilson, R.E. 1979, *ApJ*, **234**, 1054.
Wilson, R.E., and Devinney, E.J. 1971, *ApJ*, **166**, 605.
Woźniak, P. R., *et al.* 2004, *AJ*, **127**, 2436.
Yakut, K., and Eggleton, P.P. 2005, *ApJ*, **629**, 1055.
Zola, S., *et al.* 2005, *Acta Astron.*, **55**, 389.
Zola, S., Nelson, R.H., and Şenavci, H.V. 2012, *New Astronomy*, **17**, 673.